PHYSICAL REVIEW A VOLUME 27, NUMBER 6 JUNE 1983

Raman studies of argon dimers in a supersonic expansion. II. Kinetics of dimer formation

H. P. Godfried* and Isaac F. Silvera*
Natuurkundig Laboratorium der Universiteit van Amsterdam, Valckenierstraat 65, 1018 XE Amsterdam, The Netherlands
(Received 13 August 1982)

Results of a systematic study of the formation of dimers in a supersonic free-jet expansion of argon as studied by Raman scattering are presented. By seeding the expansion with N_2, measurements of temperature and density were obtained in the part of the flow field where dimers were observed. Temperature was also measured in the remaining part of the expansion showing large deviations from the behavior of an isentropic expansion due to condensation. The condensation was observed directly by Rayleigh scattering as well. From the Raman spectra it was shown that the dimers can relax their internal energy rapidly enough to come into thermal equilibrium with the translational degrees of freedom. By relating the intensity of dimer transitions to that of the simultaneously measured N_2 $J=0\rightarrow 2$ Raman transition, we were able to measure the concentration of dimers in the expansion. The measurements were compared to the predictions of equilibrium theory for a chemical equilibrium between dimers and monomers. The predictions of two- and three-body collision dimer-formation models were also tested.

I. INTRODUCTION

Since the original study of Kantrowitz and Grey[1] describing a nozzle expansion used for the production of a molecular beam, the study of the expansions themselves has developed as a complete field of physics. For the monatomic gases the gas dynamics are relatively well understood, but in expansions of polyatomic molecules the internal relaxation processes can, in most cases, only be described in a qualitative manner. This derives from the fact that the temperature-dependent rate constants are usually too difficult to calculate from first principles. However, even with a knowledge of such rate constants the gas dynamicist is faced with the problem of solving a generalized Boltzmann equation[2] that also includes the internal degrees of freedom subject to boundary conditions determined by the geometry of the expansion system. Calculations for this problem must, therefore, rely on simplifying assumptions about the magnitude of the rate constants and their behavior as a function of temperature. In addition, approximations to the flow equations must be made that make the differential equations tractable for numerical integration.[3]

In expansions in which clustering occurs, the same problems exist with increased acuity. In addition to models for the internal relaxation of the clusters a description of the formation processes would be required to reach a full understanding of the flow. Experimental input to the problem can certainly give a great stimulus to the theory of such condensing flows. Experimental observations should provide the theoretician with local values of quantities such as temperature, density, flow velocity, clustered mass fraction, etc. Some of these quantities have been measured previously with Pitot probes or by inserting a skimmer in the expansion and observing the properties of the resulting beam.[4] These techniques necessarily suffer from the inherent disturbances they introduce in the expansion. In this article we present the results of a light scattering study of an argon free-jet expansion close to the onset of condensation, where dimerization kinetics are expected to be important. The extremely weak interaction between the light and the gas particles insures that the expansion is not affected by the measurements. Onset of condensation was measured with Rayleigh scattering as a function of source pressure in expansions from room temperature. In our expansion system it was also possible to observe Raman spectra of argon dimers for the first time.[5] In a companion article[6] (to be referred to as paper I) details of the spectroscopy have been discussed. Here we shall concentrate on the gas kinetics in the system. From the spectra it was possible to determine a dimer temperature. Independent measurements of the expansion temperature were obtained

from the rotational Raman spectrum of N_2 that was seeded in low concentrations into the expansion. By relating the intensities of the dimer and N_2 spectra local values of the dimer concentrations were obtained. In this way, the first reliable determination for the dimer fraction in an expansion was made, finding $X_2 \simeq 1.4\%$.[7]

Our article is structured in the following way. First, the experimental technique is discussed. In Sec. III the Rayleigh and Raman scattering measurements of the density and temperature in the expansion are given. In Sec. IV the dimer spectra are discussed and the dimer temperature derived from them. In Sec. V the dimer concentration measurements are presented. This last section also deals with predictions of several models for the dimer density in the expansion. The separation into two kinetic parts describing relaxation (Sec. IV) and formation (Sec. V) is clearly somewhat artificial since there is a strong relation, but this increases readability.

II. EXPERIMENTAL

Details of the light scattering system were given in I. Here we shall only discuss the construction of the nozzle, the gas handling, and the experimental procedure in the Rayleigh scattering experiment.

The room-temperature nozzle had a conical inner and outer shape (angles 90° and 120°). A conical shape was necessary to minimize interference with the laser beam. In the top of the cone a 140-μm-diameter hole had been made by spark erosion. The diameter-to-length ratio was estimated to be $\lesssim 1$. The nozzle was mounted on a XYZ translation stage for alignment with respect to the laser focus and scanning of the flow field in the measurements. The small size of the laser focus (10-μm diameter) with respect to the nozzle diameter insured that local values of the measured quantities were obtained.

The argon purity was nominally 99.996%. The main impurities were N_2 and O_2. Dust filters were used in the nozzle supply line to avoid effects of inhomogeneous condensation. Maximum source pressures in this experiment were approximately 10 atm. The nozzle Reynolds number was always larger than $\sim 15\,000$ so that effects of a viscous boundary layer were negligible. Gas in the expansion chamber was pumped away by a 75-liter/sec Roots pump. Background pressures were of the order of 0.2 torr. Since no skimmer was used, the expansion could be probed upstream of the Mach disk. Its position was calculated[8] as $(X/D)_{\text{Mach}} \simeq 120$, where D is the nozzle diameter.

Rayleigh scattering was used to determine the density on the axis. For protection of the photomultiplier and to avoid effects of a changing scattering length in the argon expansion as a function of X/D, the field of view from the detector of the laser focus was limited to a boxlike volume of dimensions $\Delta X\,\Delta Y\,\Delta Z \sim 4\times 20\times 10\ \mu\text{m}^3$. X,Y,Z directions are defined by the expansion, laser, and scattered light axes, respectively.

III. DENSITY AND TEMPERATURE IN THE EXPANSION

Since the main objective of the present paper is the study of the kinetics of dimer formation and the relaxation of the energy in the internal degrees of freedom, the thermodynamic conditions in the expansion under which these kinetic processes took place were studied. Before presenting the measurements we give a qualitative description of the expansion process. First, an expansion without condensation is considered. Then, under the usual assumptions of reversible and adiabatic flow and ignoring real-gas effects, temperature and density are simply related by the isentropic relations for an ideal gas:

$$\left[\frac{\rho}{\rho_0}\right] = \left[\frac{T}{T_0}\right]^{1/(\gamma-1)} \tag{3.1}$$

with ρ the density, T the temperature, and $\gamma = c_p/c_v$. Subscripts 0 denote stagnation conditions. A relation between T and X, the position in the flow field, can, in principle, be found by solution of the hydrodynamic equations describing the isentropic flow. In practice only the hyperbolic flow equations can be solved numerically, once the boundary conditions downstream of the sonic plane are known.[9] Since the detailed shape of the nozzle determines these conditions, only simplifying assumptions are usually made about the position and shape of the sonic surface. It was shown experimentally[8] that the results of these calculations adequately describe the flow field far downstream of the nozzle throat. Deviations whose magnitudes depend on the specific boundary conditions of the experiment exist, however, at small values of X/D. In our experiment where the onset of large scale clustering occurs at $X/D \simeq 2.5$ it was important to make an experimental determination of temperature and density to avoid the uncertainties of the isentropic calculations before the onset and of the changing flow conditions caused by the unknown heat of condensation after the onset.

To show the effects of condensation we have studied the expansion with Rayleigh scattering. The intensity of the scattered light is shown in Fig. 1 as a function of X/D. The different curves correspond to different source pressures as indicated in the cap-

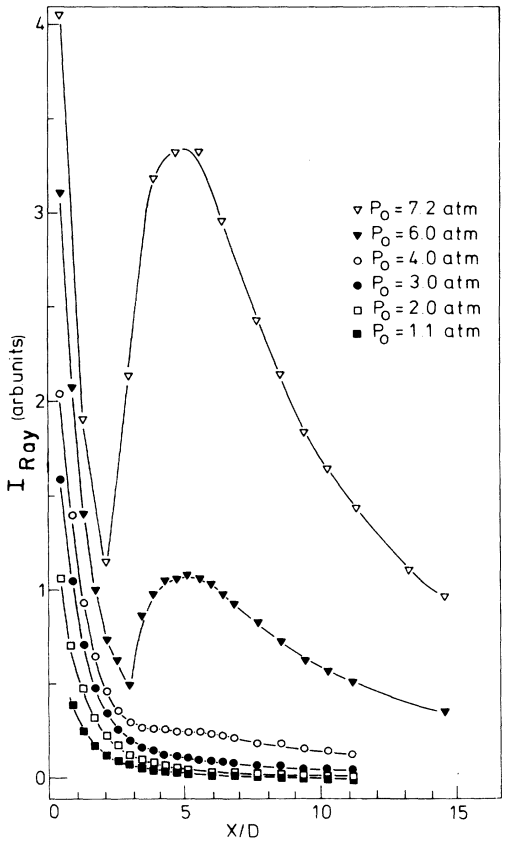

FIG. 1. Rayleigh scattering intensity as a function of X/D. Source temperature $T_0=293$ K, source pressures as indicated.

tion. For low stagnation pressures no clustering occurs. The Rayleigh signal is then just proportional to the density of atoms (monomers) and for $X/D \gtrsim 1$ the measurements agree with the predictions for an isentropic (uncondensed) free-jet expansion of a monatomic gas. For $X/D \lesssim 2.5$, the signal was in all cases approximately proportional to the pressure in the source indicating that the expansion takes place isentropically. Beyond $X/D \gtrsim 2.5$, deviations from proportionality appear for high stagnation pressures that are attributed to clustering: in an expansion with clustering the Rayleigh signal is given by

$$I_{\text{Ray}} \propto \sum_{l=1}^{\infty} \rho_l l^2 \alpha_0^2$$

with ρ_l the density of clusters consisting of l particles and α_0 the atomic polarizability. This expression ignores possible many-body effects on the polarizability. From the data in Fig. 1 it is seen that clustering increases with increasing source pressure, as expected. Although the effects of clustering are obvious, it is very difficult to interpret the results quantitatively. Very little is known about ρ_l as a function of X/D, p_0, or T_0 (T_0 is the source temperature). In previous work by Lewis *et al.*[10] on CO_2 clustering it was assumed that the monomer density was not affected by the clustering and the cluster fractions were distributed according to Poisson statistics. Such simplifying assumptions seem inappropriate in our case: The considerable heating due to cluster formation certainly affects the monomer density in the expansion even in the unlikely case where the clustered mass fraction remains small compared to the monomer fraction. The hypothesis of Poisson statistics was made *ad hoc* for want of anything better and certainly requires further study. This, however, is not attempted here.

The temperature was determined by "seeding" the expanding gas with a few percent of N_2. With the use of the rotational Raman transitions of N_2 the temperature in the expansion was measured.[11,12] This is shown in Fig. 2. Since N_2 consists of ortho and para modifications that do not interconvert in the expansion, each spectrum gives two independent measurements of the temperature. This is indicated by the open and filled data points. Circles and squares are measurement points for the Ar expansions with N_2. In addition, data are shown that were recorded on a pure N_2 expansion for calibration purposes. These measurements (indicated by △ and ▲) follow isentropic behavior for a diatomic gas with $\gamma=\frac{7}{5}$, as expected.[12,13] For the Ar expansions it is seen that the temperature follows insentropic $\gamma=\frac{5}{3}$ behavior up to the point where condensation starts according to the Rayleigh scattering data of Fig. 1. Since the rotational temperature of the seed molecules can never fall below the translational temperature of the expansion, this result directly proves the equality of the two temperatures for $X/D \lesssim 2$. Downstream of $X/D \simeq 2.5$ the temperature is essen-

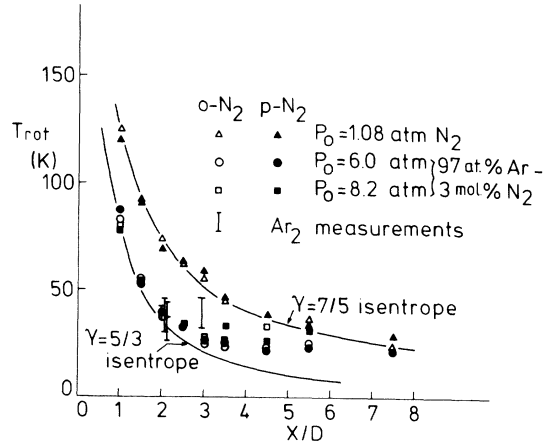

FIG. 2. Rotational temperature of nitrogen in expansions as a function of X/D.

tially constant. The coincidence of the freezing of the temperature and the onset of condensation therefore compels us to attribute the freezing to condensation and not to the rarefaction in the expansion. Since the deviations in the temperature from free-jet isentropic behavior should precede those in the density, use of the isentropic free-jet Mach number for the monomer concentration is justified upstream of the point where massive condensation starts, i.e., for $X/D \lesssim 2.5$. This means that the state of the expansion is fully determined there. We can not, however, completely ignore the effects of the formation of small clusters (see the Appendix for an estimate of the effects of dimer formation itself) on the temperature in this region. We shall exploit the above result in the discussion of the dimer kinetics by confining ourselves to the region $X/D \lesssim 2.5$. This is also motivated by the fact that it was not possible to extend the concentration measurements beyond this range. For this reason it is not necessary for the purpose of this article to explore the Rayleigh scattering further than on a qualitative basis.

IV. DIMER TEMPERATURE

In Fig. 2 the rotational temperature of N_2 seed molecules in Ar expansions is shown. Independently from these N_2 measurements a temperature could also be determined from the rotational Raman spectra of the dimers as described in I. There it was found in the fitting procedure for the temperature that the measured spectra did not deviate significantly from the generated spectra indicating the existence of a thermal distribution of the dimers in the expansion over the observed levels. The temperatures that were derived in the fitting are also given in Fig. 2. Stagnation pressure was in most cases ~ 8.2 atm. The results should, therefore, be compared to the square data points in Fig. 2. Within the experimental uncertainty there is a good agreement between the two determinations of the temperature in the expansion. This is not a trivial result: The dimers are formed in high-energy states near the dissociation limit. Relaxation must take place rapidly otherwise a nonthermal distribution would be observed. From the spectra shown in I (Figs. 3 and 4) it is seen that the molecules are indeed thermalized in the ground vibrational-rotational states and from Fig. 4 in paper I it is concluded that the occupations of the $v=1$ states are also described by a Boltzmann distribution with the same temperature. No such conclusions can be drawn, however, from these spectra for the higher vibrational states. For $v=2$ and 3 the occupations certainly are smaller than the occupation of the ground vibrational state (otherwise the observed Raman spectrum would be significantly distorted) but only upper limits can be given for their occupations (Table I, column 5). In Table I it is assumed that the rotational states within the vibrational levels are all thermalized to 39 K, the temperature observed in the spectra. No upper limits can be given from the spectra for $v > 3$.

To some extent this is possible, however, from the history of the expansion. In the following it is again assumed that thermal equilibrium exists over the rotational states for each of the vibrational states but that the vibrational degree of freedom is not necessarily thermalized. First, it is noted that for each of the vibrational states the ratio of dimers in such a state to monomers increases in an expansion of argon in which dimers and monomers are in "thermodynamic equilibrium," between 300 and 39 K. Since for a particular value v' of v, the fraction of dimers with $v > v'$ at $T=300$ K is smaller than the "equilibrium fraction" at $T=39$ K of dimers in states with $v=v'$, it is argued that the fractions of dimers in the different vibrational states cannot exceed their

TABLE I. Occupations of dimer vibrational states. Columns 2,3: equilibrium occupations at $T=39$ K. Columns 4–6: occupations relative to ground vibrational state occupation. Column 4: equilibrium values. Columns 5,6: measurements.

	P_{eq}		$P/P(0)$		
v	excl. metast.	incl. metast.	equil.	spectra	concentration
0	0.55	0.58	1	1	1
1	0.23	0.23	0.40	0.40	0.40
2	0.11	0.10	0.17	<0.40	<0.28
3	0.06	0.05	0.09	<0.40	<0.16
4	0.03	0.03	0.05		<0.09
5	0.02	0.01	0.02		<0.03

equilibrium value relative to the monomers at $T=39$ K. (Note that nothing is said about the relative occupations of the dimer levels.) At this point, we anticipate the result of Sec. V in which it is found that the occupation of the ground vibrational state $P(v=0)\geq 0.7P_{eq}(v=0)$ for the conditions of measurements ($X/D=2$ and $T=39$ K). Relative to the ground vibrational state new upper limits can thus be given (Table I, column 6). Experiments, therefore, indicate that the assumption of thermalization is quite good.

Finally, we shall try to get a feeling for the maximum gas kinetic cooling rates obtainable for the dimers and relate these to the hydrodynamic cooling rate. For this purpose, inelastic collision cross sections were calculated[14] for several representative states at $T\simeq 39$ K. Three states were chosen with the same angular momentum $J=30$: The state with $v=0$ is bound. The others with $v=2$ and 3 are metastable; the latter is strongly predissociating (paper I, Table I).

The inelastic collision cross sections were calculated as a function of the kinetic-energy change in the center-of-mass system of the collision partners. This is shown in Fig. 3. From these results the total inelastic collision cross section σ_{inel} and the second moment of the distribution were calculated.[14] The latter gives some measure of the rms energy that is exchanged in inelastic collisions. Multiplying this quantity with $\rho\langle v_{rel}\rangle\sigma_{inel}$, where $\langle v_{rel}\rangle$ is the average relative velocity, gives a measure of the maximum gas kinetic cooling rate. For the three states it was found that $\Delta E_{rms}\simeq 10$ K (Table II). With $\rho\sim 0.5$ amagat the maximum gas kinetic cooling rate would, therefore, be of the order of 10^{10} K/sec.

This result is to be compared to the hydrodynamic cooling rate in the expanding gas. The rate of change of the temperature in an isentropic expansion is easily shown to be

$$\frac{dT}{dt}=u\frac{dT}{dx}$$
$$=D^{-1}\frac{(\gamma-1)M_{is}^2}{1+\frac{1}{2}(\gamma-1)M_{is}^2}T\left[\frac{\gamma kT}{m}\right]^{1/2}\frac{dM_{is}}{dX/D}$$

with u the flow velocity, m the atomic mass, and M_{is} the isentropic Mach number. For our expansion at $X/D=2$

$$\left[\frac{dT}{dt}\right]_{hydro}\simeq 10^8 \text{ K/sec}\ .$$

Therefore, it is concluded that the dimers would have ample time to relax their energy. The preceding estimate is, however, only indicative, since only the energy exchange is considered but not the states

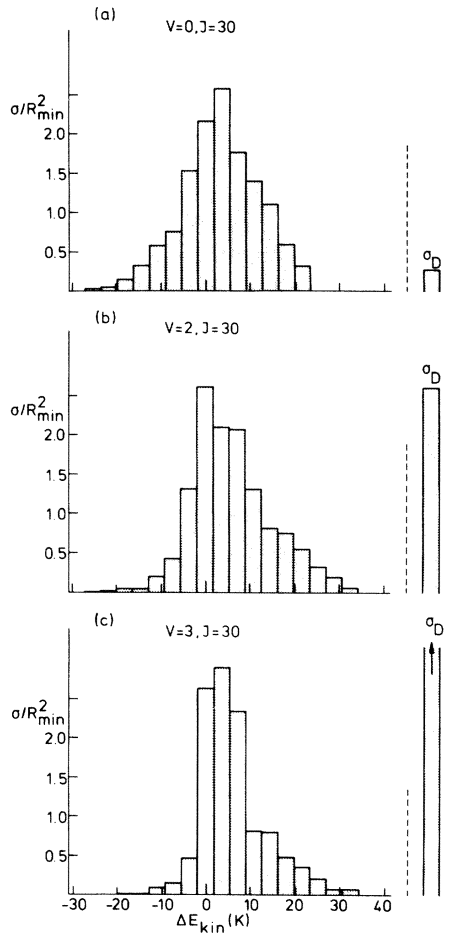

FIG. 3. Inelastic cross sections σ for argon monomer-dimer collisions at $T=39$ K as a function of the kinetic-energy change of the colliding particles. Initial dimer state: (a) $v=0$, $J=30$; (b) $v=2$, $J=30$; (c) $v=3$, $J=30$. $R_{min}=3.759$ Å is the internuclear distance at the potential minimum. σ_D is the cross section for dissociation of the dimer.

in which the dimer finds itself after the collision. Conceivably it could, therefore, be possible that the estimate of the cooling rate only applies to the rotational cooling. Therefore, cross sections for vibrational relaxation were calculated to get some more detailed information. In the calculation a dimer in the initial state $v=0$, $J=30$ collides with an atom

TABLE II. Inelastic cross sections and rms internal dimer energy change calculations at $T=39$ K (Ref. 14).

State		σ_{inel}	ΔE_{rms}
v	J	(Å^2)	(K)
0	30	189	9.3
2	30	182	10.9
3	30	178	9.5

and the cross section for a transition to a state with $v' \neq 0$ was calculated. Final values of J were not considered. Estimates for $v'=1,2$ were approximately 30 and 14 Å^2, respectively. Larger changes of v were also observed in the calculation. The corresponding transition rates are thus of the order of 10^8 sec^{-1}. Assuming the energy exchange to be again of the order of 10 K it is seen that vibrational relaxation between the lowest vibrational levels should also be rapid enough for equilibration to the monomer temperature.

From the experiments and from the estimates of obtainable cooling rates it is concluded that the dimers do reach a thermal equilibrium with the monomers for the conditions prevailing in our expansion.

V. DIMER CONCENTRATION

A. Review of earlier work

Dimer fractions have been the subject of numerous studies both experimental[15–20] and theoretical.[15,17,21,22] Dimerization was studied for widely different conditions. The experimental studies to date consist mainly of mass-spectroscopic measurements: Ion currents at the dimer and monomer masses, extracted from a molecular beam, are measured and from their ratio a dimer fraction is inferred. Uncertainties exist, however, about the ionization and fragmentation probabilities of the dimers (and larger clusters, if present). For argon this has led to reports of widely differing dimer fractions in molecular beams under comparable conditions. In early work, values were given of the order of 1% or less[15–18], with the assumption of negligible fragmentation of the dimer in the ionization process. This assumption was challenged by Lee and Fenn[19] who found considerable fragmentation in an experiment designed to test this hypothesis. As a result, they gave dimer fractions about 20 times larger than previous measurements. Subsequent experiments by Helm *et al.*[20] showed a changing fragmentation ratio as a function of electron energy, whereas Geraedts *et al.*[20] reported that fragmentation for argon dimers was negligible. This discrepancy has not been resolved to date.

Theoretical work was first mainly directed at the equilibrium dimer concentration.[15,17,21] More recently some studies were made of terminal dimer fractions from supersonic free-jet expansions.[22] Such terminal fractions could then be compared to the molecular-beam mass-spectroscopic results. In the calculation of the terminal dimer fraction, the dimer-formation processes ultimately determine the results. For argon the following two such processes have been considered.

(1) A direct three-body process in which three atoms simultaneously collide to form a stable molecule:

$$\mathrm{Ar}+\mathrm{Ar}+\mathrm{Ar} \underset{k_f}{\overset{k_r}{\leftrightarrows}} \mathrm{Ar}_2+\mathrm{Ar} \, . \tag{5.1}$$

(2) A two-step process in which, in a binary collision, an intermediate collision complex is formed. This is subsequently stabilized in a collision with a third atom:

$$\mathrm{Ar}+\mathrm{Ar} \leftrightarrows \mathrm{Ar}_2^* \, , \tag{5.2a}$$

$$\mathrm{Ar}_2^* + \mathrm{Ar} \underset{k_f}{\overset{k_r}{\leftrightarrows}} \mathrm{Ar}_2+\mathrm{Ar} \, . \tag{5.2b}$$

When discussing the present experimental results we shall return to these models and apply them to the expansion conditions of this experiment.

B. Definition of a dimer

Before going into the actual measurements of the concentration it is first useful to discuss what is meant by a dimer. More specifically, the question is raised whether or not metastable states should be included when discussing dimer concentrations. This, in fact, is determined by the experimental conditions in which the dimers are observed. In molecular-beam experiments, for instance, a distinction can be made between stable and metastable dimers. For the most part, the latter will not survive the flight through the molecular-beam apparatus because of predissociation. On the other hand, in a Raman spectroscopic investigation of their properties in an equilibrium gas, such a distinction is not very meaningful because the linewidths are generally dominated by collisional broadening which is not different for stable and metastable dimers.[6,23]

In an expansion, however, with its strong possible deviations from equilibrium, a distinction could conceivably be made from a thermodynamic point of view even in a Raman experiment. It is possible, for instance, to conceive of a situation in which metastables are rapidly formed and dissociated but stable molecules are produced at a rate which is too slow to effectively take place in the expansion or, more unlikely, the permuted situation. The first could occur if stable molecules are formed via intermediate metastable states. If the intermediates should dissociate rapidly, e.g., via tunneling, stable dimers would hardly be formed. That this situation is, in fact, extremely unlikely is again indicated by the inelastic cross-section calculations of Frenkel.[14] We have included the level widths associated with these cross sections in column 6 of Table I, paper I. The widths given are essentially equal and larger than

the natural widths of most of the tunneling states (column 4). In addition, when looking at the distribution of the energy exchanged in the inelastic collisions (Fig. 3) no qualitative differences are seen between stable and metastable molecules. It is, therefore, felt that dimer states do exchange with one another and no distinctions should be made between stable and metastable molecules. This means that in discussing the dimer concentration measurements the concentration will refer to both the stable and metastable molecules unless noted differently.

C. Results and data reduction

Although no quantitative information is obtained from the conditions for which dimer spectra were observed, it is useful to specify those conditions for the experimentalist designing a system. Stagnation pressures varied generally between 4.5 and 8.2 bar. Depending on this pressure a dimer signal could be observed between $1.5 \leq X/D \leq 3.5$. The lower limit was set by laser stray light. The upper limit varied with the source pressure and the alignment. The largest range was approximately obtained for $p_0 \simeq 6$ atm. This is an indication that dimers are consumed in the clustering beyond $X/D = 2.5$. We were, however, not able to make quantitative measurements. This was caused by the continuing rarefaction and increase in Rayleigh scattering of clusters which would decrease the dimer signal relative to the background of photomultiplier dark count and interference from the Rayleigh wings in the spectrum. In this region of the expansion where massive clusters were formed, the signal-to-noise ratio was generally too low to obtain quantitative information from the spectra. The concentration measurements that will be discussed below were, therefore, all taken in a regime where massive clustering had not yet started. Comparison of the present stagnation conditions with those of others[15–20] shows that in the other experiments care was usually taken to avoid large clustering, since fragmentation of larger clusters would contaminate the dimer signal in the mass spectrometer. A measure of the onset of this clustering was found by van Deursen,[17] who determined a limiting pressure p_L below which only dimers are formed. For our source ($D = 140$ μm and $T_0 = 293$ K) $p_L = 0.94$ atm. In fact, our stagnation pressures are so high that the dimer signal in a comparable beam experiment would decrease as a function of source pressure due to heating effects through condensation in the expansion.[17]

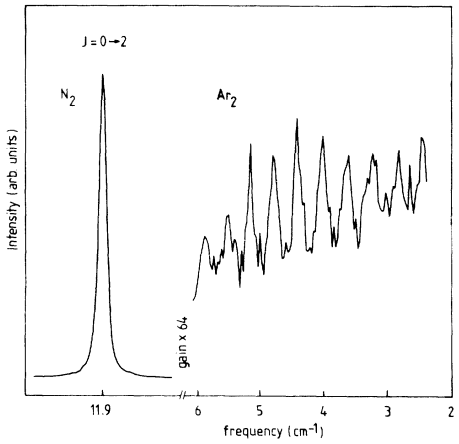

FIG. 4. Rotational spectrum of argon dimers in an N_2 seeded expansion, including N_2 $J = 0 \rightarrow 2$ transition. Spectrum was used for determination of dimer density in the expansion.

Dimer concentrations were determined in this experiment by expanding a mixture of Ar and $\sim 4\%$ N_2 (see Sec. III). This apparently does not affect the clustering in the expansion; we also assume that the dimerization is not changed by the addition of the N_2.[24] The N_2 was included as a reference gas and for the determination of the expansion temperature by means of its Raman spectrum. From the temperature measurement in this mixed expansion and from another measurement in a pure N_2 expansion, the argon monomer density was derived under the assumption of an isentropic density behavior which was shown to be valid for $X/D \lesssim 2.5$. A rotational spectrum of Ar_2 was then recorded with the high-resolution Fabry-Perot interferometer system. Simultaneously, the intensity of the N_2 $J = 0 \rightarrow 2$ transition was measured. This lies at approximately 11.9 cm^{-1} and does not interfere with the Ar_2 spectrum, as shown in Fig. 4. From the measured dimer spectrum a stick spectrum was generated with the use of the DID model (see paper I); the intensity was determined by the measured peak heights. The assumption that complete thermalization had taken place over the energy levels of the dimer was made. This provided us with a value for the dimer $J = 0 \rightarrow 2$ intensity, which, in fact, was not observed in the experiment, but is convenient to use in the analyses.

The density of Ar_2 was determined with the use of

$$\frac{I_{0\rightarrow 2}(\mathrm{Ar_2})}{I_{0\rightarrow 2}(\mathrm{N_2})} = \frac{\rho(\mathrm{Ar_2})}{\rho(\mathrm{N_2})} \left[\frac{\beta_{\mathrm{Ar_2}}}{\beta_{\mathrm{N_2}}} \right]^2 \frac{Z(\mathrm{N_2})}{Z(\mathrm{Ar_2})} \tag{5.3}$$

in which the stick value of the ground vibrational $J = 0 \rightarrow 2$ Raman transition of Ar_2 is related to the measured value of the corresponding N_2 transition.

TABLE III. Ar-dimer concentration measurements.

Case	T_0 (K)	ρ_0 (cm^{-3})	X/D	T_{seed} (K)	ρ_1 (cm^{-3})	ρ_2 (cm^{-3})	X_2	$K_{eq,0}$ (cm^3)	K_{eq} (cm^3)	K_{obs} (cm^3)
a	293	1.85×10^{20}	1.7	47.4	1.2×10^{19}	$>1.1\times10^{17}$	$>0.010\pm0.0025$	0.485×10^{-22}	0.139×10^{-20}	$>0.083\times10^{-20}$
b	293	1.5×10^{20}	2.0	39.3	6.1×10^{18}	0.88×10^{17}	0.014 ± 0.003	0.485×10^{-22}	0.235×10^{-20}	0.24×10^{-20}

β_{Ar_2} was calculated with the DID model (see paper I). $(\beta_{N_2})^2$ was taken as 0.50 Å^6,[25] and for the evaluation of the sum of states $Z(N_2)$ a value of the rotational constant $B_{N_2}=1.9895$ cm^{-1} was used.[26] The sum of states $Z(Ar_2)$ was calculated with the use of the energy levels of Colbourn and Douglas.[27] At the temperature of the expansion ($\sim$40 K) metastables made a contribution of approximately 10% to the sum. Two such measurements of the concentration are given in Table III. The relevant stagnation and expansion conditions are found in columns 2–5. The argon monomer (dimer) density is given in column 6 (7) and the dimer fraction in column 8. Discussion of the remaining quantities is postponed until after the next section.

For expansion conditions a (Table III), only lower bounds to the dimer density can be given because stray light due to reflection of the laser from the nozzle inhibited a better determination. The values given in columns 7 and 8 for conditions b differ from those that were given in Ref. 5, although they refer to the same measurements. This was caused by the use of an erroneous value of β_{N_2} taken from Ref. 28. We furthermore reexamined the assumption of an isentropic expansion made in that paper. Owing to the small deviations in the temperature from isentropic behavior [Eq. (3.1)], it was found necessary to correct the monomer density used in Ref. 5. For the dimer fraction these two corrections worked in opposite directions.

D. Equilibrium constant

Before continuing the discussion of the results we first want to go into the calculation of the equilibrium constants for the dimerization reaction. In the following we neglect the influence of larger clusters. In equilibrium theory the equilibrium constant for a chemical reaction

$$A+A\leftrightarrows A_2 \tag{5.4}$$

is given by[29]

$$K_{eq}=\frac{\rho_2}{\rho_1^2}=\left[\frac{h^2}{\pi mkT}\right]^{3/2}Z_{2,int} \tag{5.5}$$

with h Planck's constant, m the monomer mass, and $Z_{2,int}$ the internal partition function of the dimer,

$$Z_{2,int}=\sum_{v,j}(2j+1)\exp(-E_{vj}/kT)\ . \tag{5.6}$$

Several authors have reported calculations for the equilibrium constants $K_{eq}(T)$. Stogryn and Hirshfelder[21] calculated both the values of the equilibrium constant for the stable and metastable dimers for the Lennard-Jones 6-12 potential. Their results could be approximated by

$$K^s_{eq}(T)=2.520\sigma^3\left[\frac{kT}{\epsilon}\right]^{-3/2}G^s\left[\frac{kT}{\epsilon}\right] \tag{5.7a}$$

and

$$K^m_{eq}(T)=0.900\sigma^3\left[\frac{kT}{\epsilon}\right]^{-3/2}G^m\left[\frac{kT}{\epsilon}\right] \tag{5.7b}$$

with $G^s(x)=1+0.254x^{-1}+0.057x^{-2}+0.011x^{-3}$ and $G^m(x)=1-0.190x^{-1}+0.032x^{-2}-0.005x^{-3}$. Superscripts s and m denote stable and metastable contributions, respectively, and σ and ϵ are the usual Lennard-Jones repulsive-core and well-depth param-

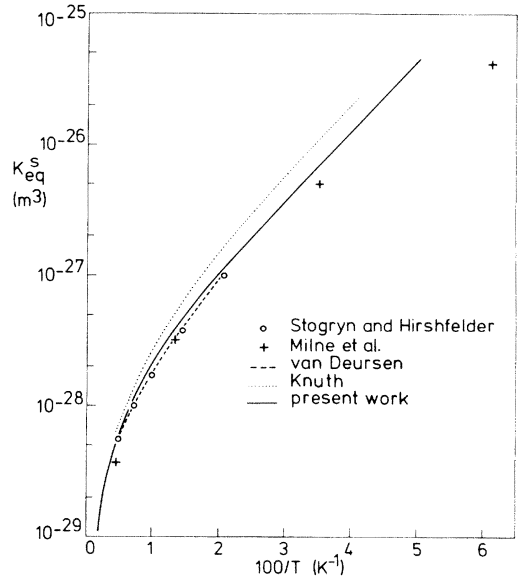

FIG. 5. Equilibrium constant K^s_{eq} for the reaction $Ar+Ar\rightleftarrows Ar_2$ as a function of inverse temperature. Only stable dimers are considered.

eters. Milne[15] used the numerical solutions of Cashion[30] for the 6-12 Lennard-Jones potential to calculate $K^s_{eq}(T)$. van Deursen[17] used the spectroscopic constants of Docken and Schafer[31] for his calculation of K^s_{eq}. In the present work the internal partition function $Z_{2,int} \equiv Z(Ar_2)$ was calculated with the spectroscopic data of Colbourn and Douglas.[27] Although obviously lacking the universality of the expression with the use of a Lennard-Jones potential, this is the most accurate calculation. Results of the different approaches are compared in Fig. 5. Because in the previous work mostly K^s_{eq} was considered, the comparison is made for that quantity. In addition to the models mentioned above we have included data points of an analytical approximation by Knuth[22] to the results of Milne. This "approximation" clearly deviates strongly from those data.

E. Discussion of results

Values of the equilibrium constant at the stagnation and local expansion temperature are given in columns 9 and 10 of Table III. In column 11 we give an observed value defined by

$$K_{obs} = \frac{\rho_2}{\rho_1^2} .$$

The values of K_{obs} and K_{eq} are seen to be equal within the experimental error for conditions b, Table III. Although this seems to indicate that the concentration of dimers is equal to the equilibrium value, it should be realized that the assumption of a thermal distribution was invoked in the calculation of the dimer density. Actually what was directly measured was the density of dimers in the ground vibrational states. From the uncertainty in the measurement and from the fact that the occupation of a state cannot exceed its equilibrium value relative to the monomers we can set boundaries on $P(v=0)$: $0.7P_{eq}(v=0) \leq P(v=0) \leq P_{eq}(v=0)$. We continue this discussion with the assumption of thermalization since we believe this to be justified in view of the measurements and cooling rate estimates as explained in Sec. IV. We can then draw some conclusions with regard to the dimer-formation process and the anisotropy of the argon-dimer polarizability.

1. Dimer formation

As mentioned in Sec. V A, dimer-formation models exist capable of predicting the terminal dimer fraction after expansion is completed by tracing the formation history during the expansion. The present local values of the concentration now can give an immediate test of these models at a stage where dimers are still being formed in the expansion. Because the present results do not suffer from the interpretation difficulties mentioned in Sec. V A and the experimental uncertainties are small, the outcome of this test should be more meaningful than the results in the mass-spectroscopic experiments.

First, the direct three-body recombination models are considered. In such a reaction [Eq. (5.1)] the rate equation is given by

$$\frac{\partial \rho_2}{\partial t} = k_f^{(3)}(\rho_1^3 - \rho_1\rho_2/K_{eq}) \tag{5.8}$$

with ρ_1 and ρ_2 the monomer and dimer densities, respectively, and k_f the forward rate constant. The backward rate constant k_r is assumed to be equal to the one in thermodynamic equilibrium (microscopic reversibility), i.e., $k_r = k_f/K_{eq}$. Taking the hydrodynamic derivative in the expansion we get

$$\frac{d\rho_2}{dX/D} = \frac{Dk_f^{(3)}}{u}\left[\rho_1^3 - \frac{\rho_1\rho_2}{K_{eq}}\right] - M\frac{dM}{dX/D}\left[1+\frac{\gamma-1}{2}M^2\right]^{-1}\rho_2 . \tag{5.9}$$

This equation was numerically integrated. The Mach number was assumed to be equal to its value for an isentropic expansion, M_{is}. The analytic form of Ashkenas and Sherman[8] was used to which an exponential was joined for $X/D < 1$ with matched values and derivative at $X/D = 1$. A complication arose from the fact that the temperature in our expansion started to show deviations from isentropic behavior when it had reached a value of 39 K. This was programmed in by "freezing" T at 39 K downstream of where the experiment showed deviations. This procedure contains the implicit assumption, justified from our measurements, that while condensation does heat up the expansion, there are still no direct effects on the dimer concentration: the latter can still be described by a formation-dissociation equilibrium with monomers only.

For $k_f^{(3)}$ two models have been proposed based on mass-spectroscopic measurements by Milne *et al.*[15] and Golomb *et al.*[16] Milne *et al.* proposed an inverse power-law dependence of k_f on T:

$$k_f^{(3)} = B_n/T^n . \tag{5.10}$$

Such a form has also been observed in reactions involving chemically bound diatomic molecules.[32] Optimum correlations were found for $2 \lesssim n \lesssim 3$. The predictions of these models with $n = 2, 3$ are shown in Fig. 6 for the expansion conditions b in Table III.

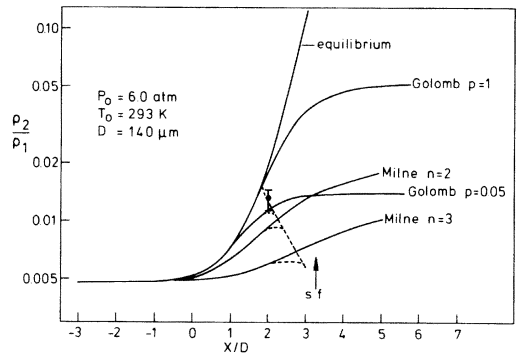

FIG. 6. Model calculations for dimer fraction as a function of X/D for the expansion conditions b of Table III. Solid lines are calculated for an isentropic expansion; dashed lines give results for expansion in which heating due to condensation keeps temperature constant downstream of $X/D \simeq 1.8$. Data point corresponds to the measured fraction.

The model clearly fails to reproduce the equilibrium concentration at $X/D=2$. In this model, as Knuth pointed out, most of the increase in the dimer fraction takes place in the outer part of the expansion. The low temperatures attained there enhance the formation process in this model so much that, in spite of the rarefaction, dimers continue to be formed and the formation process actually needs to be cut off. This was done by Milne at the translational sudden-freeze surface.[33]

Golomb *et al.*[16] proposed the use of the three-body collision rate[34] multiplied by some factor q describing the effectiveness of the collision

$$k_f^{(3)}=8\pi^{3/2}\sigma^5\left[\frac{kT}{m}\right]^{1/2}q \tag{5.11}$$

with $q=pe^{-E/kT}$. The factor q was taken to be 1, resulting in the (unphysical) model that every three-particle collision produces a bound dimer. Even for this high value of q the model predicted lower final dimer concentrations than the experimental observations. Predictions of this model for our expansion conditions are included in Fig. 6. The model agrees with the measured dimer concentration. Therefore, the steric factor p was reduced keeping the activation energy E equal to 0 to find a lower bound for p. A value of $p_{\text{low}} \simeq 0.05$ was found for conditions b, Table III. Another estimate was obtained by taking $E \simeq 0.6\epsilon$ with ϵ the potential-well depth. This seems a reasonable value in view of the fact that the maximum rotational barrier in a two-particle description is approximately 0.8ϵ. We found $p_{\text{low}} \simeq 0.2$. It is noted that when applying the model with these values of p_{low} and E to the expansions of Ref. 16 the final dimer fractions would be much lower than the observed values. If the model provides a good description of the dimer formation process for $p \simeq p_{\text{low}}$, this would indicate that the dimer detection probability in mass spectrometers is substantially higher (approximately ten times) than previously assumed. Such a large factor seems rather improbable. It is, therefore, felt that the model does not give a consistent description of the available experimental data for such low values of p.

Finally, a two-step model is considered. Knuth[22] has studied a model in which dimers are formed via stabilization of unbound (virtual orbiting) pairs of atoms. Other possible reaction paths via metastable states were ignored on the basis of a statistical argument. Knuth then found the rate limiting process to be the stabilization of the unbound pairs. A sudden-freeze model was developed in which the dimer-formation process is assumed to be in equilibrium up to the sudden-freeze surface where the dimerization is discontinuously interrupted. The position of this surface is determined by the rate limiting process. The formation rate is then given by

$$\frac{\partial\rho_2}{\partial t}=k_f^{(2)}(\rho_2^*\rho_1-\rho_2\rho_1/K_{\text{eq}}^*) \tag{5.12}$$

with

$$k_f^{(2)}=\pi\sigma_{A-A_2^*}^2\Omega^{(2,2)}\left[\frac{12}{\pi}\frac{kT}{m_A}\right]^{1/2}q\ .$$

ρ_2^* is the (equilibrium) concentration of unbound pairs. $\sigma_{A-A_2}^*$ is a hard-sphere collision diameter and $\Omega^{(2,2)}$ the normalized collision integral. The collision effectiveness q is again assumed to be of Arrhenius form:

$$q=pe^{-E/kT}\ .$$

The equilibrium constant K_{eq}^* is now the equilibrium constant for the process

$$\mathrm{Ar}_2^*+\mathrm{Ar}\underset{k_f}{\overset{k_r}{\rightleftarrows}}\mathrm{Ar}_2+\mathrm{Ar}\ .$$

This model was not numerically integrated as was done for the direct process. Only the location $(X/D)_{\text{sf}}$ of the sudden-freeze (sf) surface was calculated with the use of Knuth's results (Ref. 22, Eq. 42), again ignoring effects of formation of larger clusters:

$$T_{\text{sf}} \simeq 18\text{K},\quad (X/D)_{\text{sf}}=3.3\ .$$

The prediction of an equilibrium concentration at $X/D=2$, therefore, agrees with the experiments presented here. It is noted, however, that the use by

Knuth of too large a value of the equilibrium constant K_{eq} (see Fig. 5) increases the value of $(X/D)_{sf}$. The magnitude of this shift is difficult to estimate due to the complicated form of the model.

2. *Dimer polarizability*

In I the dimer polarizability was discussed and in the calculation of the density the dimer polarizability results of the DID model (see I) were used. Several other models were also considered in I. From the spectroscopy we could not, however, decide whether or not any of these other models was acceptable. From the present concentration measurements this is possible. We recall the relations

$$I \propto \beta^2 \rho_2$$

and

$$\rho_2 \leq \rho_{2eq} .$$

From these relations and the experimentally determined Raman intensity one can set a lower bound on the value of β^2. Using the DID model for β we found that, within the error bounds, $\rho_2 \geq 0.7\rho_{2eq}$. Therefore, we find

$$\beta^2 \geq 0.7\beta^2_{DID} ,$$

$$|\beta| \geq 0.84\beta_{DID} .$$

Comparing this result to Table III of paper I we find that models 2–5 and 8 can be rejected. Our results agree with the recent collision-induced light scattering data[35] in that corrections to the DID model are small.

VI. SUMMARY OF RESULTS

In this article a consistent description was given of the dimer-formation process in an argon free-jet expansion. Measurements of temperature and density were presented that established the conditions in which dimers are formed in our expansion. These Rayleigh and Raman scattering results also proved the existence of an isentropic expansion core down to the region where condensation starts. From Raman scattering on dimers it was possible to conclude that dimers are in thermal equilibrium with monomers. This means that the internal energy of the dimers corresponds to the local translational temperature of the expansion. The dimer concentration was found to be equal to the value it would have in a chemical equilibrium with monomers, neglecting the direct influence of larger clusters on the equilibrium. The local values of the concentration obtained here were compared to predictions of a few dimer-formation models that were suggested in the literature. The two-step formation model of Knuth and the three-body collision model of Golomb *et al.* could give results in agreement with the experiments. The other models considered did not give acceptable results. With the use of the present density measurements a lower bound was found for the anisotropic polarizability of the argon dimer.

ACKNOWLEDGMENTS

We thank G. M. van Waveren for assistance with the measurements, and Dr. D. Frenkel for the use of his inelastic collision cross-section calculations. Financial support of the Stichting Fundamenteel Onderzoek der Materie is gratefully acknowledged.

APPENDIX

In this appendix we want to estimate the effects of dimer formation in the "isentropic" part of the expansion $X/D \lesssim 2.0$ on the temperature. Thermal equilibrium is assumed and the classical expressions for equipartition are used: the energy of the free rotating, vibrating dimer is taken as $2kT$. This means that at $X/D \simeq 2$ where isentropic temperature is ~ 35 K, internal dimer energy is ~ 70 K and the average energy needed to dissociate the dimers is ~ 75 K. Multiplying with the dimer fraction ($\sim 1.5\%$) we get the total heat per dimer in the expansion delivered to the translational bath in the dimer-formation process. This value is to be compared to the average thermal kinetic energy in the flowing system of ~ 54 K. Therefore, the increase in the translational temperature due to the dimer formation is of the order of 0.8 K.

---

*Address after 1 September 1982: Lyman Laboratory of Physics, Harvard University, Cambridge, MA 02138.

[1]A. Kantrowitz and J. Grey, Rev. Sci. Instrum. 22, 333 (1951).

[2]L. Waldmann, in *Handbuch der Physik,* edited by S. Flügge (Springer, Berlin, 1958), Vol. XII.

[3]H. Rabitz and S.-H. Lam, J. Chem. Phys. 63, 3532 (1975).

[4]See, e.g., O. Hagena, in *Molecular Beams and Low Density Gas Dynamics,* edited by P. P. Wegener (Dekker, New York, 1974), Ch. 2.

[5]H. P. Godfried and I. F. Silvera, Phys. Rev. Lett. 48, 1337 (1982).

[6]H. P. Godfried and I. F. Silvera, Phys. Rev. A 27, 3008

(1983), referred to as paper I.

[7]This value differs from the value quoted in Ref. 5. There we used a value of 0.86 $Å^6$ for the square of the anisotropy in the polarizability taken from Ref. 28. We subsequently discovered that this value is incorrect (Ref. 25) and should be 0.50 $Å^6$. See Sec. V C for a further discussion of this problem.

[8]H. Ashkenas and F. S. Sherman, *Proceedings of the Fourth International Symposium on Rarefied Gas Dynamics, Toronto, 1964,* edited by J. H. de Leeuw (Academic, New York, 1966), p. 84.

[9]P. L. Owen and C. K. Thornhill, Aeronautical Research Council United Kingdom, Report No. RM-2616 (unpublished); also J. B. Anderson, in *Molecular Beams and Low Density Gas Dynamics,* edited by P. P. Wegener (Dekker, New York, 1974).

[10]J. W. L. Lewis, W. D. Williams, and H. M. Powell, *Proceedings of the Ninth International Symposium on Rarefied Gas Dynamics, Göttingen, 1974,* edited by M. Becker and M. Fiebig (Deutsche Forschungs-und Versuchsanstalt für Luft-und Raumfahrt, Porz-Wahn, West Germany, 1974), Vol. II, p. F7.

[11]I. F. Silvera and F. Tommasini, Phys. Rev. Lett. 37, 136 (1976); I. F. Silvera, F. Tommasini, and R. J. Wijngaarden, *Proceedings of the Tenth International Symposium on Rarefied Gas Dynamics, Aspen, 1976,* edited by J. L. Potter (AIAA, New York, 1977), Vol. II, p. 1295.

[12]G. Luijks, S. Stolte, and J. Reuss, Chem. Phys. 62, 217 (1981).

[13]D. Coe, F. Robben, L. Talbot, and R. Cattolica, *Proceedings of the 11th International Symposium on Rarefied Gas Dynamics, Cannes, 1978,* edited by R. Campargue (Commissariat à l'Energie Atomique, Paris, 1979), Vol. II, p. 907.

[14]D. Frenkel (private communication).

[15]T. A. Milne, A. E. Vandergrift, and F. T. Greene, J. Chem. Phys. 52, 1552 (1970).

[16]D. Golomb, R. E. Good, and R. F. Brown, J. Chem. Phys. 52, 1545 (1970).

[17]A. P. M. van Deursen, Ph.D. Thesis, University of Nijmegen, 1976 (unpublished).

[18]R. M. Yealland, J. M. Decker, J. D. Scott, and C. T. Tuori, Can. J. Phys. 50, 2464 (1972).

[19]N. Lee and J. B. Fenn, Rev. Sci. Instrum. 49, 1269 (1978).

[20]H. Helm, K. Stephan, and T. D. Märk, Phys. Rev. A 19, 2154 (1979); J. Geraedts, S. Setiadi, S. Stolte, and J. Reuss, unpublished work.

[21]D. E. Stogryn and J. O. Hirshfelder, J. Chem. Phys. 31, 1531 (1959).

[22]E. L. Knuth, J. Chem. Phys. 66, 3515 (1977).

[23]D. Frenkel and J. P. McTague, J. Chem. Phys. 70, 2695 (1979).

[24]T. A. Milne and F. T. Greene, J. Chem. Phys. 47, 4095 (1967); See Fig. 7.

[25]F. Baas and K. D. van den Hout, Physica (Utrecht) 75A, 597 (1979); C. M. Penney, S. T. Peters, and M. Lapp, J. Opt. Soc. Am. 64, 712 (1974); N. J. Bridge and A. D. Buckingham, Proc. R. Soc. London, Ser. A 295, 334 (1966).

[26]*Topics in Current Physics: Raman Spectroscopy of Gases and Liquids,* edited by A. Weber (Springer, Berlin, 1979), Ch. 3.

[27]E. A. Colbourn and A. E. Douglas, J. Chem. Phys. 65, 1741 (1976).

[28]J. O. Hirshfelder, C. F. Curtiss, and R. B. Bird, *Molecular Theory of Gases and Liquids* (Wiley, New York, 1954).

[29]T. L. Hill, *Introduction to Statistical Mechanics* (Addison-Wesley, Reading, Mass., 1960), Ch. 10.

[30]J. K. Cashion, J. Chem. Phys. 48, 94 (1968).

[31]K. K. Docken and T. P. Schafer, J. Mol. Spectrosc. 46, 454 (1973).

[32]J. F. Clarke and M. McChesney, *Dynamics of Relaxing Gases* (Butterworths, London, 1976), Ch. 5.

[33]J. B. Anderson and J. B. Fenn, Phys. Fluids 8, 780 (1965).

[34]A. A. Frost and R. G. Pearson, *Kinetics and Mechanism* (Wiley, New York, 1963), p. 69.

[35]D. P. Shelton and G. C. Tabisz, Can. J. Phys. 59, 1430 (1980); also, L. Frommhold, in *Advances in Chemical Physics,* edited by I. Prigogine and S. A. Rice (Wiley, New York, 1981), Vol. 46.